Dalton Transactions

Accepted Manuscript

This is an *Accepted Manuscript*, which has been through the Royal Society of Chemistry peer review process and has been accepted for publication.

Accepted Manuscripts are published online shortly after acceptance, before technical editing, formatting and proof reading. Using this free service, authors can make their results available to the community, in citable form, before we publish the edited article. We will replace this *Accepted Manuscript* with the edited and formatted *Advance Article* as soon as it is available.

You can find more information about *Accepted Manuscripts* in the Information for Authors.

ROYAL SOCIETY OF CHEMISTRY

www.rsc.org/dalton

Journal Name Dalton Transactions Dynamic Article Links ►

Cite this: DOI: 10.1039/c0xx00000x

www.rsc.org/xxxxxx

ARTICLE TYPE

Syntheses, crystal structures, MMCT and magnetic properties of four one-dimensional cyanide-bridged complexes comprised of M^{II}-CN-Fe^{III} (M = Fe, Ru, Os)

Yong Wang,[a,b] Xiao Ma,[a] Shengmin Hu,[a] Yuehong Wen,[a] Zhenzhen Xue,[a,b] Xiaoquan Zhu,[a,b] Xudong Zhang,[a] Tianlu Sheng*,[a] and Xintao Wu[a]

Received (in XXX, XXX) Xth XXXXXXXXX 20XX, Accepted Xth XXXXXXXXX 20XX
DOI: 10.1039/b000000x

Four new one-dimensional (1D) zigzag chain cyanide-bridged complexes [*cis*-$M^{II}(L)_2(CN)_2Fe^{III}$(salen)]($PF_6$) (M = Fe, L = bpy, **3**; M = Fe, L= phen, **4**; M = Ru, L = bpy, **5**; M = Os, L = bpy, **6**) (bpy = 2, 2'-bipyridine, phen = 1, 10-phenanthroline, salen = N, N'-ethylenebis(salicylideneaminato) dianion) have been synthesized and characterized structurally as well as magnetically, especially **3** and **4** are mixed-valence complexes. Fortunately, the crystals of complexes **3, 4** and **6** suitable for single-crystal X-ray diffraction analysis were obtained. Also, the electronic absorption spectra indicate the existence of the MMCT (metal-to-metal charge transfer) bands in complexes **3-6**. Temperature dependent magnetic susceptibilities reveals that the Fe(III)-Fe(III) exchange coupling separated by diamagnetic cyanidometal -NC-M(II)-CN- bridge is weak ferromagnetic for **3-5**, but weak anti-ferromagnetic for **6**. What'more, the specific heat measurements suggest complexes **3-5** exhibit a phase transition at 2.8 K, 2.7 K and 2.6 K, respectively.

Introduction

Mixed-valence (MV) compounds have attracted considerable attention for more than 40 years, this mainly stems from their interesting MMCT[1] and magnetic properties.[2, 3] A great variety of MV complexes have been prepared, and are playing an important role in areas including multi-electron donor/acceptor systems,[4] magnetic properties,[5] photo-induced electron transfer,[6] and for understanding electronic delocalization between metal centers from a fundamental standpoint.[7, 8] Especially, one-dimensional (1D) chain MV metal complexes have fascinated physicists and chemists in the context of molecular electronics owing to their potential application as "molecular wires".[9] In the MV chemistry, the investigation on cyanide-bridged MV compounds has grown to be a major-research effort. Prussian blue, $Fe^{III}_4[Fe^{II}(CN)_6]_3$, represents the oldest examples[10] and exhibits MMCT band[11] at 14100 cm^{-1} and weak ferromagnetic coupling[12]. However, 1D cyanide bridged MV complexes are scarcely investigated[13] because of the difficulty in preparing such complexes and especially in obtaining suitable crystals for molecular structure analysis.

Most recently, we have focused on the investigation of MMCT and/or magnetic properties of cyanide bridged MV compounds.[14, 15] In this work, four 1D zigzag chain cyanide-bridged complexes, [*cis*-$M^{II}(L)_2(CN)_2Fe^{III}$(salen)]($PF_6$) (M = Fe, L = bpy, **3**; M = Fe, L= phen, **4**; M = Ru, L = bpy, **5**; M = Os, L = bpy, **6**), were synthesized by reaction of diamagnetic precursors $M^{II}(L)_2(CN)_2$ with $Fe^{III}(salen)^+$ in the presence of NH_4PF_6. Herein, the syntheses, crystal structures, IR, MS, elemental analysis, electronic absorption spectroscopy and magnetic properties of these complexes will be described in detail.

Experimental Methods

Physical measurements

Elemental analyses (C, H, N) were performed at a Vario MICRO elemental analyzer. Mass spectra (MS) were collected on DECAX-30000 LCQ Deca XP Ion Trap mass spectrometer using DMF (N, N-dimethylformamide) as the mobile phase. Infrared (IR) spectra were obtained from KBr pellets with a Perkin-Elmer Spectrum One FT-IR spectrophotometer. Electronic absorption spectra were measured on a Perkin-Elmer Lambda 900 UV-vis-NIR spectrophotometer in a quartz cell (1 cm). ^{1}H NMR spectra were recorded on a RUKER BIOSPIN AVANCE III 400 MHz spectrometer in appropriate solvents at ambient temperature. Solution was contained in standard 5 mm sample tubes. Chemical shifts are reported in δ (ppm), relative to internal TMS for ^{1}H NMR spectra. Temperature dependence magnetic susceptibilities were carried out using a Quantum Design Magnetic Property Measurement System (MPMS) SQUID-XL. Specific heat measurements were conducted on a Physical Property Measurement System (PPMS) PPMS-9T. Diamagnetic corrections of complexes **3-6** were estimated from Pascal's Tables. The diamagnetic susceptibilities are -505.1×10^{-6} cm^3 mol^{-1} K for **3**, -551.1×10^{-6} cm^3 mol^{-1} K for **4**, -520.1×10^{-6} cm^3 mol^{-1} K for **5** and -536.1×10^{-6} cm^3 mol^{-1} K for **6**, respectively.

Materials and syntheses

All manipulations were performed under argon atmosphere with the use of standard Schlenk techniques unless otherwise depicted. Acetonitrile was dried by distillation over calcium hydride under argon atmosphere. Methanol was dried by distillation over magnesium. DMF was dried by distillation over $MgSO_4$. *cis*-$Fe^{II}(bpy)_2(CN)_2{\cdot}3H_2O$[16, 17] (**1**), *cis*-$Fe^{II}(phen)_2(CN)_2{\cdot}2H_2O$[16, 17], *cis*-$Ru^{II}(bpy)_2(CN)_2{\cdot}2H_2O$[18], *cis*-$Os^{II}(bpy)_2Cl_2$[19] and $[Fe^{III}(salen)](NO_3)$[20] were prepared according to the literature procedures. All other reagents were available commercially and used without further purification.

cis-$Os^{II}(bpy)_2(CN)_2{\cdot}7H_2O$, 2

This complex was prepared according to a modified method based on the previous report.[21, 22] 20 equivalents of KCN (2275 mg, 35.0 mmol) was added to a solution of *cis*-$Os^{II}(bpy)_2Cl_2$ (1000 mg, 1.74 mmol) in water (100 ml), and then the mixture was refluxed for additional 8 h, during which time the solution gradually changed from red-brown to black-brown and some brown precipitate appeared. After cooled to room temperature, the brown precipitate was collected by filtration and washed with water, 2-propanol and ethyl ether, respectively. After drying in air, the desired brown product (696 mg, 59%) was obtained. Brown crystals of **2** suitable for X-ray diffraction were obtained by evaporation of the methanol solution of **2** in air. ^{1}H NMR (CD_3OD, δ/ppm) 9.68 (d, J = 5.6, 2H), 8.41 (dd, J = 24.4, 8.4 Hz, 4H), 7.85 (dt, J = 7.8 Hz,1.2Hz, 2H), 7.75 (dt, J = 8.0Hz, 1.2Hz, 2H), 7.46 (dt, J = 6.1 Hz, 1.2Hz, 4H), 7.15 (dt, J = 6.6 Hz,1.2Hz, 2H). Anal. Calcd for $OsC_{22}H_{16}N_6{\cdot}7H_2O$: C, 38.82, H, 4.44; N, 12.35%. Found: C, 38.82; H, 4.36; N, 12.27%. IR (KBr pellet, cm^{-1}): 2057 (CN), 2040(CN). UV-vis (CH_3CN), $\lambda_{max,}$ nm (ε, dm^3 mol cm^{-1}): 336 (11870), 372 (11569), 445 (10667), 496 (13074), 650 (3370). MS, m/z: 555.1[**2**+H]$^+$.

[*cis*-$Fe^{II}(bpy)_2(CN)_2Fe^{III}(salen)](PF_6){\cdot}DMF{\cdot}CH_3CN{\cdot}H_2O$, $3{\cdot}DMF{\cdot}H_2O{\cdot}CH_3CN$

A solution of *cis*-$Fe^{II}(bpy)_2(CN)_2{\cdot}3H_2O$ (100 mg, 0.211 mmol) in methanol (25ml) was mixed with 1.1 equiv of $[Fe^{III}(salen)](NO_3)$ (89.0 mg, 0.232 mmol) at room temperature. The reaction mixture was heated to 60 °C and stirred under argon atmosphere for 6 h, resulting in a purple solution. Solid NH_4PF_6 (37.8 mg, 0.232mmol) was then added to the above reaction solution. A red-purple precipitate appeared immediately and was collected (144 mg, 67%). Deep purple crystals of **3** suitable for X-ray diffraction were obtained by a mixed solution of DMF (5 ml), CH_3CN (5 ml) and diethyl-ether (30 ml). Anal. Calcd $Fe_2C_{38}H_{30}N_8O_2PF_6{\cdot}DMF{\cdot}H_2O$: C, 50.33, H, 4.02; N, 12.88%. Found: C, 50.27; H, 4.00; N, 12.39%. IR (KBr pellet, cm^{-1}): 2085 (CN), 2067 (CN). UV-vis (CH_3CN), λ_{max}, nm (ε, dm^3 mol cm^{-1}): 356 (12900), 528 (6570), 609 (3434). MS, m/z: 742.0 [**2**-PF_6]$^+$.

[*cis*-$Fe^{II}(phen)_2(CN)_2Fe^{III}(salen)](PF_6){\cdot}2DMF{\cdot}H_2O$, $4{\cdot}2DMF{\cdot}H_2O$

Compound **4** was prepared by using the same procedure as for compound **3**, except for the addition of *cis*-$Fe^{II}(phen)_2(CN)_2{\cdot}2H_2O$ (106 mg, 0.211 mmol) instead of *cis*-$Fe^{II}(bpy)_2(CN)_2{\cdot}3H_2O$. Yield red-purple solids (132 mg, 57%). Anal. Calcd for $Fe_2C_{42}H_{30}N_8O_2PF_6$: C, 53.93; H, 3.23; N, 11.98%. Found: C, 53.54; H, 3.69; N, 12.53%. IR (KBr pellet, cm^{-1}): 2102(CN), 2087 (CN). UV-vis (CH_3CN), λ_{max}, nm (ε, dm^3 mol cm^{-1}): 372 (14952), 512 (6825), 595 (3584). MS, m/z: 790.9[**4**-PF_6]$^+$.

[*cis*-$Ru^{II}(bpy)_2(CN)_2Fe^{III}(salen)](PF_6)$, 5

Compound **5** was prepared by using the same procedure as for compound **3**, except for the addition of *cis*-$Ru^{II}(bpy)_2(CN)_2{\cdot}2H_2O$ (106 mg, 0.211 mmol) instead of *cis*-$Fe^{II}(bpy)_2(CN)_2{\cdot}3H_2O$. Yield brown solids (122 mg, 62%). Anal. Calcd for $RuFeC_{38}H_{30}N_8O_2PF_6$: C, 48.94; H, 3.24; N, 12.02%. Found: C, 48.25; H, 3.44; N, 11.91%. IR (KBr pellet, cm^{-1}): 2084(CN), 2053(CN). UV-vis (CH_3CN), λ_{max}, nm (ε, dm^3 mol cm^{-1}): 328(16210), 461(10244), 495(8856). MS, m/z: 788.1[**5**-PF_6]$^+$.

[*cis*-$Os^{II}(bpy)_2(CN)_2Fe^{III}(salen)](PF_6)$, 6

Compound **6** was prepared by using the same procedure as for compound **3**, except for the addition of *cis*-$Os^{II}(bpy)_2(CN)_2{\cdot}7H_2O$ (144 mg, 0.211 mmol) instead of *cis*-$Fe^{II}(bpy)_2(CN)_2{\cdot}3H_2O$. Yield brown-black solids (121mg, 56%). Anal. Calcd for $OsFeC_{38}H_{30}N_8O_2PF_6$: C, 44.67; H, 2.96; N, 10.97%. Found: C, 44.39; H, 3.10; N, 11.02%. IR (KBr pellet, cm^{-1}): 2068 (CN), 2028 (CN). UV-vis (CH_3CN), λ_{max}, nm (ε, dm^3 mol cm^{-1}): 333(17170), 472(11205), 514(10545), 617(3613), 712(1977). MS, m/z: 878.1[**6**-PF_6]$^+$.

X-Ray structure determination

The single crystal data for complexes **3, 4** and **6** were collected on Saturn724+ CCD diffractometer equipped with graphite-monochromatic Mo K_α (λ = 0.71073 Å) radiation by using an ω-scan model technique at 123 K. In order to compare the change of related bond lengths, the single crystal data for complexes **1** and **2** were collected under the same condition. All the structures were solved by the direct method using *SHELXS-97*[23] and refined by full-matrix least-squares techniques on F^2 with *SHELXL*-97. Anisotropic thermal parameters were used for the non-hydrogen atoms, and isotropic thermal parameters were used for the hydrogen atoms. Hydrogen atoms were calculated geometrically and refined using a riding model to the attached atoms. Crystallographic data and structural refinement details for complexes **1-4** and **6** are summarized in Table 1, and selected bond distances and bond angles are provided in Table 2.

CCDC-1015599 (**1**), CCDC-1015600 (**2**), CCDC-1015601 (**3**), CCDC-1015602 (**4**), CCDC-1015603 (**6**) contain the supplementary crystallographic data, related bond lengths and angles for this paper. These data can be obtained free of charge from The Cambridge Crystallographic Data Centre via www.ccdc.cam.ac.uk/data_request/cif.

Results and Discussion

Synthesis

Complex **2** was prepared according to the literature procedure in a straightforward way by refluxing of *cis*-$Os^{II}(bpy)_2Cl_2$ and extremely excess KCN (20 equiv.) in water for 8 h.

Evaporating of the CH_3OH solution of **2** led to brown crystals, which were characterized by IR, electronic absorption spectra, elemental analysis, ^{1}HNMR, MS and single-crystal X-ray diffraction analysis. The crystals suitable for single-crystal X-ray diffraction analysis of *cis*-$Fe^{II}(bpy)_2(CN)_2$ (**1**) were obtained in the same way as complex **2**.

Reaction of *cis*-$M^{II}(L)_2(CN)_2$ (M = Fe, Ru, Os; L = bpy, phen) with equivalent molar of $[Fe^{III}(salen)](NO_3)$, respectively, in the presence of NH_4PF_6 afforded a series of 1D zigzag chain complexes [*cis*-$M^{II}(L)_2(CN)_2Fe^{III}(salen)](PF_6)$ (M = Fe, L = bpy, **3**; M = Fe, L = phen, **4**; M = Ru, L = bpy, **5**; M = Os, L = bpy, **6**). Fortunately, red-purple to blown-black crystals of complexes **3**, **4** and **6** suitable for single-crystal X-ray diffraction analysis were obtained. All complexes **3-6** were characterized by IR, MS, elemental analysis and electronic absorption spectroscopy. The M^+ ion peak in the mass spectra and the matching elemental analysis confirmed compounds **3-6**.

Description of the crystal structures of 1-6

Both complexes **1** and **2** are simple zero dimensional mononuclear molecular square and crystallizes in monoclinic space group $P2_1/n$, $C2/c$, respectively (Figure 1)**.** **1** contains two uncoordinated water solvent molecules, complex **2** contains seven uncoordinated water solvent molecules. As shown in Figure 1, both compounds **1** and **2** adopt a distorted $[MC_2N_4]$ octahedral coordination, in which four coordination sites around the metal centers are occupied by four nitrogen atoms from two bpy ligands and the other two sites are occupied by two carbon atoms from the cyanide bridges in an *cis*-position.

Complexes **3**, **4**, **6** are all 1D zigzag chain compounds. Compounds **3** and **4** crystallize in monoclinic space group $P2_1/n$, and compound **6** crystallizes in monoclinic space group $C2/c$. Complex **3** contains one DMF, one CH_3CN and one H_2O solvent molecules, and complex **4** contains two DMF and one H_2O solvent molecules, while complex **6** contains no solvent molecule. Complexes **3**, **4** and **6** possess 1D chain cationic structures composed of repeated [-NC-$M^{II}(L)_2(\mu$-CN)Fe^{III}(salen)-] unit with one positive charge balanced by one PF_6^- anion. Because the crystal structures of complexes **3**, **4** and **6** are similar, here only the structure of complexes **3** is described in detail. As shown in Figure 2, the repeat unit of complex **3** consists of $Fe^{II}(bpy)_2(CN)_2$ and $[Fe^{III}(salen)]^+$ fragments. Every two $[Fe^{III}(salen)]^+$ fragments are bridged by $Fe^{II}(bpy)_2(CN)_2$ in an *cis*- conformation, and every two $M^{II}(bpy)_2(CN)_2$ fragments are bridged by $[Fe^{III}(salen)]^+$ in a *trans*-conformation, resulting in a 1D [-NC-M^{II}-CN-Fe^{III}-]$_n$ chain. Unlike the bond angles of Fe-C≡N (177.4(5)° and 177.1(5)°) are nearly linear, the bond angles of Fe-N≡C(CN) (159.6(5)° and 168.6(4)°) are deviated significantly from linearity. The selected bond distances and bond angels are listed in Table 2. The bond distances of M^{II}-C(CN) in **3** (1.867(6)-1.889(6) Å) are shorter than that of **6** (1.967(9)-1.977(7) Å). The bond distances of M^{II}-N(bpy) increase from 1.965 (5)-1.996(5) Å in **3** and 1.970(3)-2.002(3) Å in **4** to 2.064(8)-2.123(7) Å in **6**. Also, the $M^{II}\cdots Fe^{III}$ distance in **3** (av. 5.079Å) and **4** (av. 5.139Å) are shorter that in **6** (av. 5.207Å). These behaviors can be contributed to the larger metal radii of Os^{II} than that of Fe^{II}.

Similar to other salen-based complexes,[25] the packing of bimetallic chains is often dominated by aromatic π-π stacking interactions. For compounds **3-6** the chains are running along the *b* direction, and the chains form layers parallel to the *bc* plane. (Figures S1-S3 in Supporting Information). Moreover, the shortest distances between two neighboring chains are 4.03 Å (**3**), 3.86 Å (**4**) and 3.97 Å (**6**), which were longer than the common stacking distance of about 3.4 to 3.6 Å[26], suggesting the interactions between the adjacent chains can be neglected in complexes **3-6**. The intrachain shortest $Fe^{III}\cdots Fe^{III}$ separated by -NC-M^{II}-CN- are 6.830 (**3**), 6.897 (**4**) and 6.680 Å (**6**).The nearest $Fe^{III}\cdots Fe^{III}$ distances between the adjacent chains are 11.5 (**3**), 12.2 (**4**) and 11.7 Å (**6**), indicating the interchain interaction between the Fe^{III} ions can be ignored.

IR spectroscopy

The cyanide stretching frequencies data for **3-6** and related precursors are listed in Table 3. For cyanide-bridged complexes the ν_{CN} stretching vibrations are very representative. Three factors are considered to affect the cyanide stretching frequency for the fromation of cyanide-bridged complex: (i) kinematic coupling; (ii) back-bonding from the N-bonded metal; iii) back-bonding from the C-bonded metal.[27] Herein there are two ν_{CN} IR bands for complexes **3-6** and related cyanide precursors., which are the combination of symmetric and asymmetric stretching frequencies in *cis*- complexes. It can be found that the ν_{CN} of the cyanide-bridged complexes (**3-6**) are higher than that of related cyanide precursors. This could be attributed to the former two factors in dominant, that is both kinematical coupling occurring when a second metal is attached to the CN unit and the fact that the cyanide N donated electron density from an anti-bonding molecular orbital to the Fe(III) centre, thereby increasing the CN force constant.

From the ν_{CN} stretching vibrations of the corresponding Fe, Ru and Os complexes it can be found that the following two trends are obvious: the separation between the two ν_{CN} increases and both the two ν_{CN} bands move to low frequencies in the series of Fe < Ru < Os. This is due to the increase of the d(M)-π*(CN) back-bonding interaction in the order of Fe < Ru < Os.[28, 29] These results are consistent with the detail study of mononuclear complexes reported by *A. A. Schilt* [28].

Electronic absorption spectroscopy and MMCT

The electronic absorption spectra of complexes **3-6** and their precursors were measured in the CH_3CN solution at room temperature and shown in Figures 4-7 and S4-S7, and the data for the related complexes are listed in Table 3. The electronic absorption spectra of the related precursors *cis*-$Fe^{II}(bpy)_2(CN)_2\cdot 3H_2O$[16, 21, 22, 30], *cis*-$Fe^{II}(phen)_2(CN)_2\cdot 2H_2O$,[16, 30] *cis*-$Ru^{II}(bpy)_2(CN)_2\cdot 2H_2O$,[21, 22] and *cis*-$Os^{II}(bpy)_2(CN)_2\cdot 7H_2O$[21, 22] have been investigated by other chemists. The bands near 581nm in *cis*-$Fe^{II}(bpy)_2(CN)_2\cdot 3H_2O$, 580 nm in *cis*-$Fe^{II}(phen)_2(CN)_2\cdot 2H_2O$, 483 nm in *cis*-$Ru^{II}(bpy)_2(CN)_2\cdot 2H_2O$ and 496 nm in *cis*-$Os^{II}(bpy)_2(CN)_2\cdot 7H_2O$ were assigned to $t_2(M^{II})\rightarrow\pi^*(L)$

MLCT (metal-to-ligand charge transfer) band.[22] And the band in 650 nm of $Os^{II}(bpy)_2(CN)_2 \cdot 7H_2O$ should be attributed to the ^{3}MLCT[31] due to the low symmetry splitting of the metal level and the stronger spin-orbit coupling in Os^{II} than in Ru^{II} and Fe^{II}.[32, 33]

After forming the cyanide bridged Fe^{II}-CN-Fe^{III} complex, the maximum absorption band moves from 581 nm of $Fe^{II}(bpy)_2(CN)_2$ to 528 nm of complex **3**. This shift of the MLCT may be due to the stabilization of the d(Fe) orbitals by the presence of an electron acceptor (Fe(III)) upon forming Fe^{II}-CN-Fe^{III}. Such blue shifted behavior was also observed in complexes **4-6**, also this has been studied intensively by others.[34] The ^{3}MLCT band is also blue-shifted from 650 nm in $Os^{II}(bpy)_2(CN)_2 \cdot 7H_2O$ to 617 nm in **6**. The maximum absorption wavelength of MLCT for complexes **3-6** increases in the order: Ru (461 and 495 nm in **5**) < Os (472 and 514 nm in **6**) < Fe (528 nm in **3**). The similar phenomenon has also been reported and investigated.[22, 35] This could be explained by metal-ligand interactions and spin-orbit coupling.[33]

Besides, it can be found a new band in the electronic absorption spectra of **3** (609 nm), **4** (595 nm), and **6** (712 nm), which could be assigned to M^{II} (M = Fe or Os) to Fe^{III} electron transfer (MMCT). From the absorption band shape of 500-750 nm of **5** and its precursors, it can be speculated that there should exit a MMCT band in **5** but may be overlapped by the MCLT band at 500 nm region. Similar to the Prussian blue, $Fe^{III}_4[Fe^{II}(CN)_6]_3$, the MMCT of **3-6** should results from the t_{2g} orbital of low-spin M^{II} ion to t_{2g} orbital of high-spin Fe^{III} ion through the bridging cyanide ligand.[11] The MMCT bands in complexes **3, 4** and **6** are analogous to those electron transfer from the low-spin Fe^{II} ion to the high-spin Fe^{III} of other systems[3, 11] For **3** and **4**, the MMCT occurs in the same metal atoms and the intensity of MMCT band is strongest.

Based on the above MMCT band shape[7] and the related Fe^{III}-N bond distances, the mixed valence complexes **3** and **4** are assigned to partial delocalization and should belong to the Class II mixed valence complexes, according to the classification of Robin and Day.[36]

Magnetic properties

The variable-temperature magnetic susceptibilities of solid samples of **3** and **4** were collected under an external magnetic field of 1000 Oe using a SQUID magnetometer range 2-300 K in Figures 8-9. The $\chi_M T$ values at 300 K are 4.83 cm^3 K mol^{-1} for **3** and 4.81 cm^3 K mol^{-1} for **4**, which are slightly higher than the expected theoretical values of 4.375 cm^3 K mol^{-1} for one uncoupled high-spin (HS) Fe(III)[37] ($S_{Fe(III)}$ = 5/2) and one diamagnetic low-spin (LS) Fe(II) ions ($S_{Fe(II)}$ = 0) assuming g = 2.0 due to a significant orbital contribution from Fe(III) ions.[38] As the temperature is lowed, the $\chi_M T$ values keep nearly a constant value until about 22 K for **3** and about 32 K for **4**, and then start to decrease smoothly, reaching a minimum value of 4.75 cm^3 K mol^{-1} for **3** and 4.43 cm^3 K mol^{-1} for **4** at about 9 K. Below 9 K, the $\chi_M T$ values rapidly increased with further decreasing temperature to 6.86 cm^3 K mol^{-1} for **3** and 4.99 cm^3 K mol^{-1} for **4** at 2 K, probably suggesting a phase transition.[39] The magnetic data of both **3** and **4** between 10 K to 300 K obey the Curie-Weiss law, $\chi_M = C/(T-\theta)$, affording θ = 0.75 K, C = 4.76 cm^3 K mol^{-1} for **3** and θ = 0.19 K, C = 4.81 cm^3 K mol^{-1} for **4**. The positive θ values, together with the shape of the curves of χ_M-T and $\chi_M T$-T, indicate the presence of weak ferromagnetic coupling between the Fe(III) ions through the diamagnetic cyanidometal -NC-Fe(II)-CN- bridge in **3** and is stronger than that in **4**. This suggests phen is a stronger π-acceptor compared to bpy.

On the basis of the molecular structure, the magnetic susceptibility for complex **3** is fitted by the following equation with Hamiltonian: $\mathbf{H} = -2J\,\Sigma\,\mathbf{S}_1 \cdot \mathbf{S}_2$. To evaluate the strength of Fe(III)-Fe(III) magnetic coupling (J) separated by the diamagnetic cyanidometal -NC-M(II)-CN- bridge, $\chi_M = Ng^2\beta^2/(kT) \times (A+Bx^2)/(1+Cx+Dx^3)$,[40] with $x = |J|/kT$, where all the symbols have their usual meaning. For the HS Fe(III) ion (S = 5/2), the value of A, B, C, D are 2.9167, 208.04, 15.543, 2707.2, respectively.[40] The best fit values obtained by the above equation are J = 0.029 cm^{-1}, g = 2.09 and $R = (\Sigma(\chi_{calcd}T - \chi_{obsd}T)^2)/\Sigma(\chi_{obsd}T)^2 = 8.7\times10^{-3}$ for complex **3**. As the fitting for **4** is not well, the result of **4** has not been showed here.

In order to further characterize the low-temperature magnetic behaviors of **3** and **4**, the specific heat of powder pellet samples **3** and **4** were measured with a zero-field by a relaxation method in the temperature range of 2-50 K. The plots of Cp^{-1} *vs.* T are given in Figure 10. The curves of Cp^{-1}-T show a peak at 2.8 K for **3** and 2.7 K for **4**, respectively, which corresponds to a phase transition at low temperature of **3** and **4**. This phase transition could also explain the sudden decreasing of $\chi_M T$ value of complex **3** and **4** at low temperature.

The variable-temperature magnetic susceptibilities of solid samples **5** and **6** were collected under an external magnetic field of 1000 Oe using a SQUID magnetometer range 2-300 K in Figures 11-12. The $\chi_M T$ values at 300 K are 4.66 cm^3 K mol^{-1} for **5** and 4.35 cm^3 K mol^{-1} for **6**, which are close to the spin-only coupled values of 4.375 cm^3 K mol^{-1} for one isolated HS Fe(III) ($S_{Fe(III)}$ = 5/2) and one isolated diamagnetic LS M(II) ($S_{M(II)}$ = 0) ions on the basic of g = 2.0. Upon cooling, the $\chi_M T$ value decreased smoothly and linearly until 30 K for **5** and until 14 K for **6**, then sharply increased to 5.22 cm^3 K mol^{-1} for **5** at 2 K, and decreased to 3.84 cm^3 K mol^{-1} for **6** at 2 K. The magnetic behavior of the linear decrease of $\chi_M T$ values with decreasing temperature indicate an extra temperature-independent paramagnetic (TIP) contribution of **5** and **6** owing to the spin-orbit coupling of paramagnetic HS Fe(III).[41] Also the specific heat of powder pellet sample **5** was measured with a zero-field by a relaxation method in the temperature range of 2-50 K. The plots of Cp^{-1} *vs.* T are given in Figure 13. The curves of Cp^{-1}-T show a peak at 2.6 K for **5**, which corresponds to a phase transition at low temperature of **5**.

To evaluate the Curie-Weiss constants of complexes **5** and **6**, a TIP ($N\alpha$) should be added to the Curie-Weiss law. By using the equation, $\chi_M = C/(T-\theta) + N\alpha$, the related parameters were obtained as follows: C = 4.25 cm^3 K mol^{-1}, θ = 0.37 K, $N\alpha = 1.59\times10^{-3}$ cm^3 mol^{-1} for **5** and C = 4.02 cm^3 K mol^{-1}, θ = -0.088 K, $N\alpha = 1.60\times10^{-3}$ cm^3 mol^{-1} for **6**. The Weiss constants, together with the magnetic behaviors, indicate a

weak ferromagnetic coupling for complex **5**, and a weak anti-ferromagnetic coupling for complex **6**. An acceptable model for the temperature dependent magnetic susceptibilities of **5** and **6** are similar to that of **3**, but a TIP should be added to the above equation for complex **5** and **6**, $\chi_M = Ng^2\beta^2/(kT)\times(A+Bx^2)/(1+Cx+Dx^3)+N\alpha$. The best-fit parameters obtained are J = 0.020 cm^{-1}, g = 1.98, R = 3.5×10^{-4} and $N\alpha$ =1.18×10^{-3}cm^3 mol^{-1} for complex **5** and J = -0.009 cm^{-1}, g = 1.93, R = 2.1×10^{-4} and $N\alpha$ = 9.0×10^{-4} cm^3 mol^{-1} for complex **6**.

It has been reported that the magnetic properties of M1-L-M2 depends on the angle of M1-L-M2.[42] For the magnetic superexchange between paramagnetic Fe(III) ions mediated by the Fe^{III}-N≡C-M^{II}-C≡N-Fe^{III} pathway involving the diamagnetic LS–M(II) centers, the magnetic coupling between paramagnetic Fe(III) ions are related to the shape of the Fe^{III}-N≡C-M^{II}-C≡N-Fe^{III} bridge.[15] For complexes **3**, **4** and **6**, the magnetic properties of Fe1-N1≡C1-M1-C2≡N2-Fe2 depend on the angle of C1-M1-C2, Fe1-N1≡C1, N1≡C1-M1, M1-C2≡N2 and C2≡N2-Fe2. It was found that the angles of C1-M1-C2, N1≡C1-M1 and M1-C2≡N2 are very close in complexes **3**, **4** and **6**, and the angles of Fe1-N1≡C1 and C2≡N2-Fe2 decrease in the order of **3**>**4**>**6**. The bending of Fe1-N1≡C1 and C2≡N2-Fe2 should result in the different magnetic behavior of complex **6**.

Conclusions

In summary, a series of new 1D zigzag chain cyanide-bridged complexes **3-6** were synthesized by reaction of diamagnetic cyanide precursors *cis*-M^{II}(L)$_2$(CN)$_2$ with [Fe^{III}(salen)]$^+$ in the presence of NH_4PF_6. What's more, complexes 3 and 4 are mixed-valence complexes. Complexes **3-6** were confirmed by MS, IR, elemental analysis, electronic absorption spectra and magnetic measurements. The electronic absorption spectra exhibits the presence of the M^{II}→Fe^{III} MMCT band in complexes **3-6**. The magnetic data indicate **3-5** are weak ferromagnetic coupling, and **6** is anti-ferromagnetic coupling. The specific heat measurements suggest a phase transition occurring at 2.8 K, 2.7 K and 2.6 K for **3-5**.

Acknowledgments

We thank 973 Program (2012CB821702 and 2014CB845603), the National Science Foundation of China (21073192, 21173223 and 21233009) for financial support.

Table 1. Details of the crystallographic Data collection, Structural Determination, and refinement for complexes **1- 6**.

	1·2H$_2$O	**2**·7H$_2$O
Chemical formula	$C_{22}H_{16}FeN_6O_2$	$C_{22}H_{16}N_6O_7Os$
Formula weight	452.26	666.61
Colour and Habit	Purple prism	Brown prism
Crystal Size (mm)	0.487×0.322×0.214	0.268×0.147×0.135
T (K)	123	123
Crystal system	monoclinic	monoclinic
Space group	$P2_1/n$	$C2/c$
a (Å)	9.257(8)	26.832(3)
b (Å)	16.127(13)	14.7225(10)
c (Å)	13.836(11)	14.7702(12)
α (deg)	90.00	90.00
β (deg)	94.234(16)	112.366(5)
γ (deg)	90.00	90.00
V (Å^3)	2060(3)	5395.9(8)
Z	4	8
ρ_{calcd} (g/cm^3)	1.458	1.641
λ (Mo K_α, Å)	0.71073	0.71073
μ (Mo K_α, mm^{-1})	0.764	4.775
Completeness	99.1%	95.1%
F (000)	928	2576
h, k, l, range	-11≤h≤12, -20≤k≤20, -17≤l≤17	-34≤h≤34, -19≤k≤19, -18≤l≤19
θ range(deg)	2.53-27.54	2.72-27.48
Reflections measured	4698	5880
R_{int}	0.0827	0.0543
Params/restraints/Data(obs.)	270/0/2925	325/18/5617
GOF	0.917	1.058
R_1, ωR_2 [$I > 2\sigma(I)$]	0.0650, 0.1639	0.0552, 0.1642
R_1, ωR_2 (all data)	0.0863, 0.1779	0.0569, 0.1664

	3·DMF·H$_2$O·CH$_3$CN	**4**·2DMF·H$_2$O	**6**
Chemical formula	$C_{43}H_{40}F_6Fe_2N_{10}O_4P$	$C_{48}H_{44}F_6O_5Fe_2N_{10}P$	$C_{38}H_{30}F_6FeO_2N_8OsP$
Formula weight	1017.52	1097.60	1021.72
Colour and Habit	Purple prism	Purple prism	Brown prism
Crystal Size (mm)	0.178×0.144×0.094	0.300×0.250×0.200	0.452×0.329×0.177
T (K)	123	123	123
Crystal system	monoclinic	monoclinic	monoclinic
Space group	$P2_1/n$	$P2_1/n$	$C2/c$
a (Å)	16.088(8)	16.747(7)	27.291(11)
b (Å)	13.258(6)	13.494(5)	12.386(5)
c (Å)	21.990(11)	22.504(10)	24.808(10)
α (deg)	90.00	90.00	90.00
β (deg)	108.196(9)	105.667(7)	105.893(6)
γ (deg)	90.00	90.00	90.00
V (Å^3)	4456(4)	4897(4)	8065(5)
Z	4	4	8

ρ_{calcd} (g/cm^3)	1.517	1.489	1.683
λ (Mo Kα, Å)	0.71073	0.71073	0.71073
μ (Mo Kα, mm^{-1})	0.767	0.706	3.619
Completeness	99.7%	99.7%	99.6%
F (000)	2084	2252	4008
h, k, l, range	-19≤h≤19, -15≤k≤15, -26≤l≤26	-21≤h≤21, -17≤k≤13, -29≤l≤29	-35≤h≤35, -15≤k≤16, -32≤l≤32
θ range (deg)	2.03-25.00	3.20-27.50	2.10-27.42
Reflections measured	7825	11222	9159
R_{int}	0.0759	0.0558	0.0782
Params/restraints/Data(obs.)	595/54/4989	704/40/7108	593/129/7398
GOF	1.017	1.033	1.070
R_1, ωR_2 [$I > 2\sigma(I)$]	0.0787, 0.2127	0.0644, 0.1300	0.0633, 0.1674
R_1, ωR_2 (all data)	0.1117, 0.2429	0.1109, 0.1570	0.0770, 0.1805

$R_1 = \Sigma||F_o| - |F_c||/\Sigma|F_o|$. $\omega R_2 = [\Sigma[w(F_o^2 - F_c^2)^2]/\Sigma[w(F_o^2)^2]]^{1/2}$.

Table 2. Selected Bond Distances (Å) and Bond Angles (°) for Complexes **1-6.**

	1	**2**
M^{II}-C1$_{cyano}$	1.901(4)	2.006(7)
M^{II}-C2$_{cyano}$	1.912(4)	1.987(8)
C1≡N1	1.174(5)	1.143(10)
C2≡N2	1.161(5)	1.163(11)
M^{II}-N3$_{pyridine}$	2.000(3)	2.112(5)
M^{II}-N4$_{pyridine}$	1.959(3)	2.069(5)
M^{II}-N5$_{pyridine}$	1.957(3)	2.064(5)
M^{II}-N6$_{pyridine}$	1.992(3)	2.089(6)
C1$_{cyano}$-M^{II}-C2$_{cyano}$	88.57(16)	90.8(3)
N1≡C1-M^{II}	178.8(3)	173.8(8)
N2≡C2-M^{II}	178.7(3)	175.0(5)

	3	**4**	**6**
M^{II}-C1$_{cyano}$	1.867(6)	1.890(4)	1.978(7)
M^{II}-C2$_{cyano}$	1.889(6)	1.886(4)	1.968(9)
C1≡N1	1.163(7)	1.157(5)	1.170(10)
C2≡N2	1.162(7)	1.152(5)	1.157(10)
M^{II}-N3$_{pyridine}$	1.996(5)	2.002(3)	2.123(7)
M^{II}-N4$_{pyridine}$	1.965(5)	1.970(3)	2.064(8)
M^{II}-N5$_{pyridine}$	1.985(5)	1.972(3)	2.065(7)
M^{II}-N6$_{pyridine}$	1.978(5)	1.996(3)	2.114(7)
Fe^{III}-N1$_{cyano}$	2.109(5)	2.183(3)	2.248(7)
Fe^{III}-N2$_{cyano}$	2.086(6)	2.152(4)	2.242(8)
Fe^{III}-N7$_{salen}$	2.144(5)	2.060(4)	1.989(7)
Fe^{III}-N8$_{salen}$	2.113(6)	2.063(3)	1.990(6)
Fe^{III}-O1$_{salen}$	1.924(5)	1.896(3)	1.876(6)
Fe^{III}-O2$_{salen}$	1.911(4)	1.893(3)	1.899(5)
C1$_{cyano}$-M^{II}-C2$_{cyano}$	87.7(2)	87.03(16)	87.7(3)
N1≡C1-M^{II}	177.4(5)	176.1(3)	177.6(6)
N2≡C2-M^{II}	177.1(5)	176.5(4)	176.4(9)
C1≡N1-Fe^{III}	159.6(5)	159.2(3)	145.1(6)
C2≡N2-Fe^{III}	168.6(4)	167.2(3)	160.1(7)
N2$_{cyano}$-Fe^{III}-N1$_{cyano}$	173.94(19)	173.52(13)	172.4(3)
M^{II}···$Fe1^{III}$	5.048	5.127	5.133
M^{II}···$Fe2^{III}$	5.111	5.151	5.281
$Fe1^{III}$ ···$Fe2^{III}$	6.830	6.897	6.680

Table 3. Cyanide stretching frequencies and electronic absorption spectra for complexes**1-5** and the related precursors.

Compound	ν_{CN} (cm^{-1})	λ_{max} / nm (ε /dm^3 mol^{-1} cm^{-1})
1	2069, 2079[43]	382(6252),581(6204)
cis-Fe(phen)$_2$(CN)$_2$·2H$_2$O	2067, 2079[44]	322(2761), 363(1284), 490(17105), 580(10226)
cis-Ru(bpy)$_2$(CN)$_2$·2H$_2$O	2062, 2078[45]	346(9428), 483(10385)[45]
2	2040, 2057	336(11870), 372(11569), 445(10667), 496(13074), 650(3370)
Fe(salen)(NO$_3$)	—	377(11892)
3	2067, 2085	356(12900), 528(6570), 609(3434)
4	2087, 2102	372(14952), 512(6825), 595(3584)
5	2053, 2084	328(16210), 461(10244), 495(8856)
6	2028, 2068	333(17170), 472(11205), 514(10545), 617(3613), 712(1977)

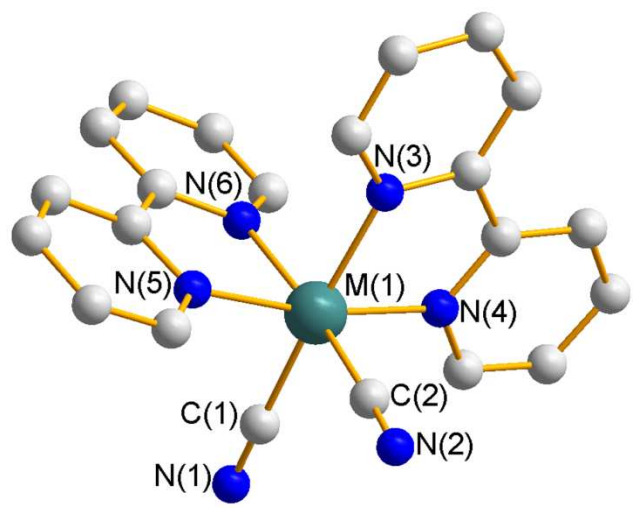

Figure 1 Crystal structure of mononuclear precursors *cis*-M(bpy)$_2$(CN)$_2$ (M = Fe, Os) . Hydrogen atoms and solvent molecular have been omitted for clarity.

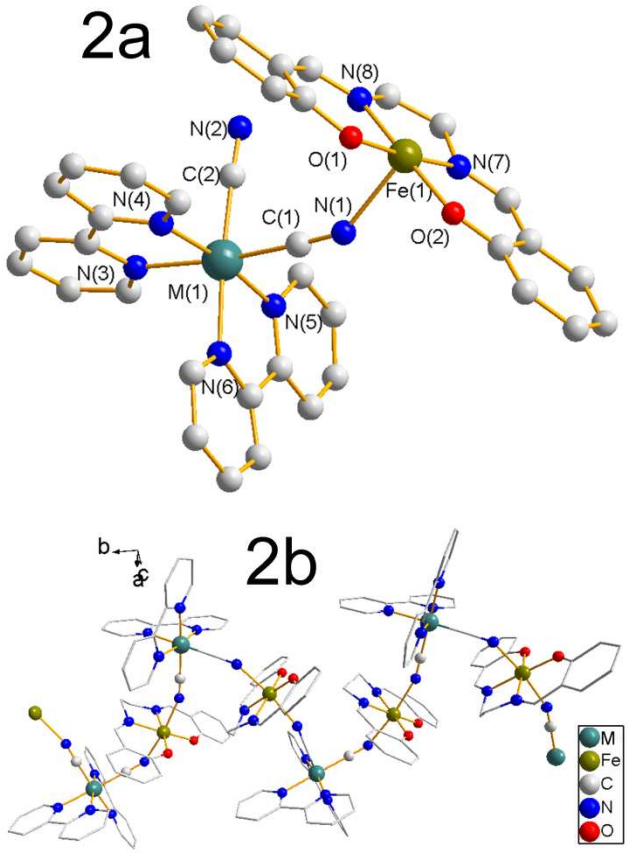

Figure 2 (2a) Crystal structure of complexes [*cis*-M(bpy)$_2$(CN)$_2$Fe(salen)](PF$_6$) (M = Fe, **3**; M = Os, **6**), (2b) Side perspective drawing of 1D chain of complexes [*cis*-M(bpy)$_2$(CN)$_2$Fe(salen)](PF$_6$). Hydrogen atoms, PF$_6^-$ anion and solvent molecular have been omitted for clarity.

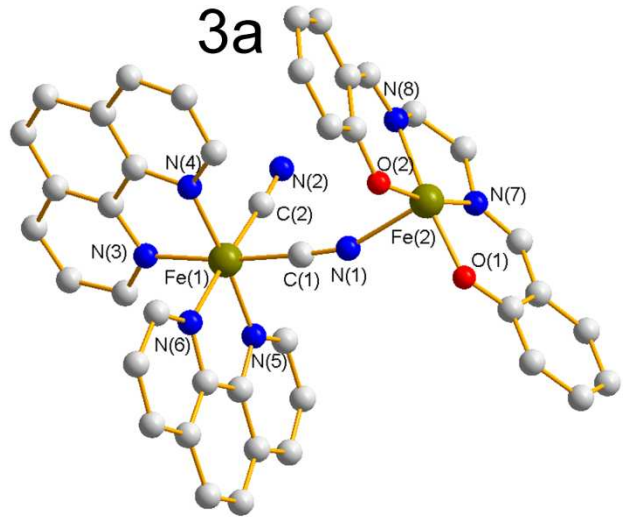

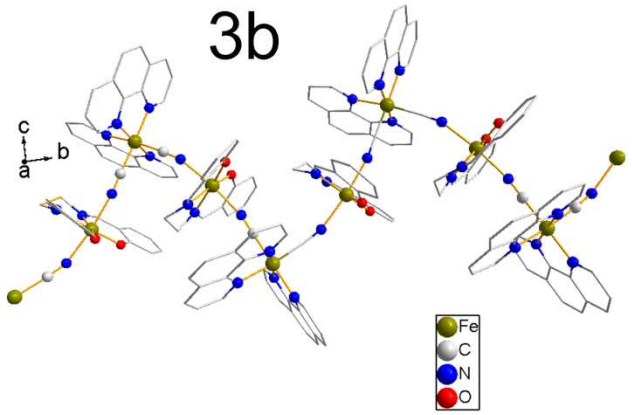

Figure 3 (3a) Crystal structure of [*cis*-Fe(phen)$_2$(CN)$_2$Fe(salen)](PF$_6$). (3b) Side perspective drawing of 1D zigzag chain of [*cis*-Fe(phen)$_2$(CN)$_2$Fe(salen)] (PF$_6$). Hydrogen atoms, the PF$_6^-$ anion and solvent molecule have been omitted for clarity.

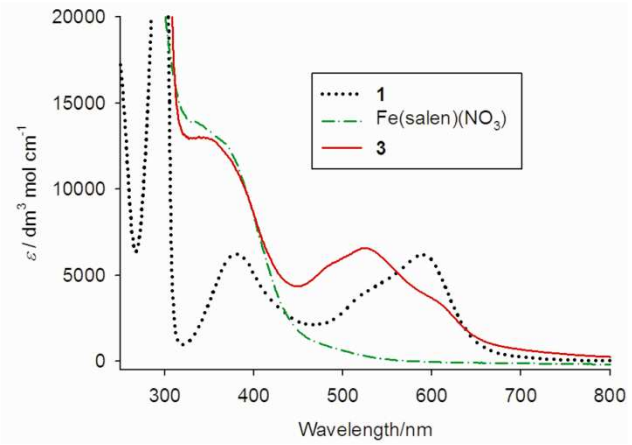

Figure 4 Electronic absorption spectra of complex **3** and related precursors in CH$_3$CN solution at room temperature.

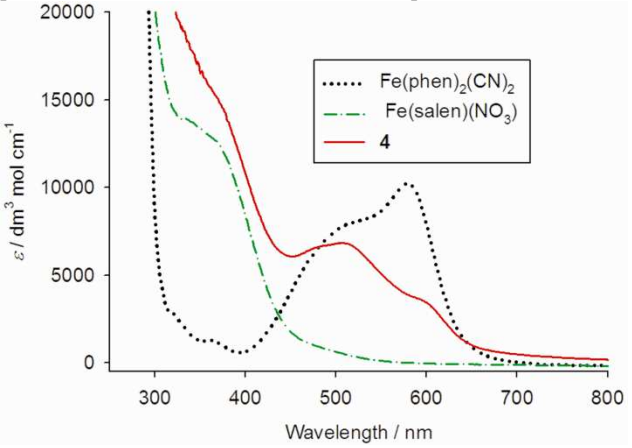

Figure 5 Electronic absorption spectra of complex **4** and related precursors in CH$_3$CN solution at room temperature.

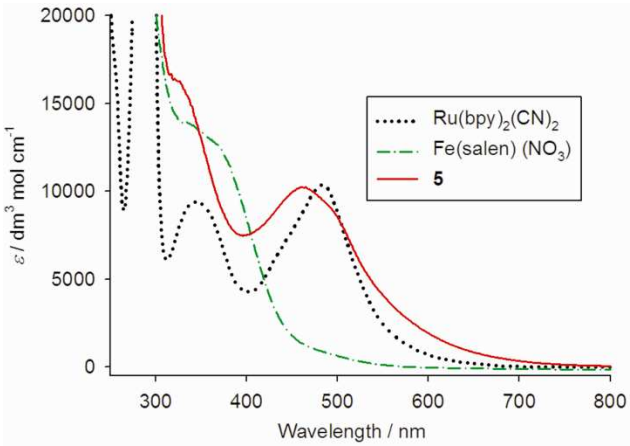

Figure 6 Electronic absorption spectra of complex **5** and related precursors in CH_3CN solution at room temperature.

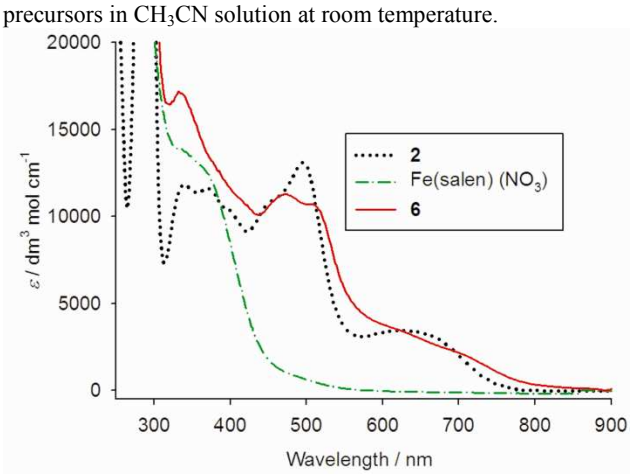

Figure 7 Electronic absorption spectra of complex **6** and related precursors in CH_3CN solution at room temperature.

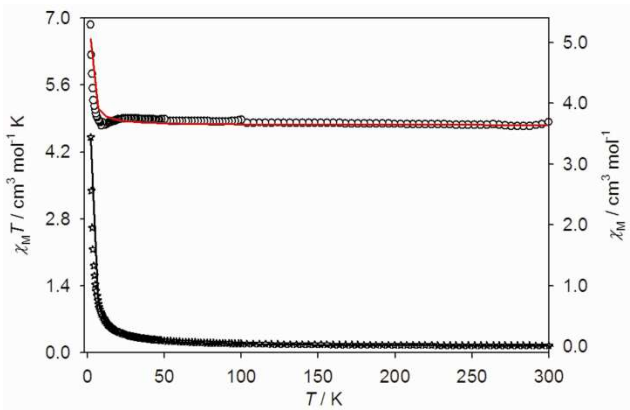

Figure 8 Magnetic behavior of complex **3** as measured in an applied field of 1000 Oe using a SQUID magnetometer. Fitting (black line) on χ_M *vs* T (star) and fitting (red line) on $\chi_M T$ *vs* T (circle) of complex **3** in the powder state.

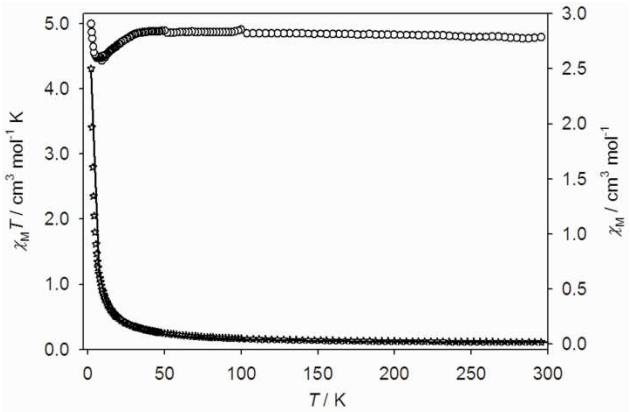

Figure 9 Magnetic behavior of complex **4** as measured in an applied field of 1000 Oe using a SQUID magnetometer. Fitting (black line) on χ_M *vs* T (star) and $\chi_M T$ *vs* T (circle) of complex **4** in the powder state.

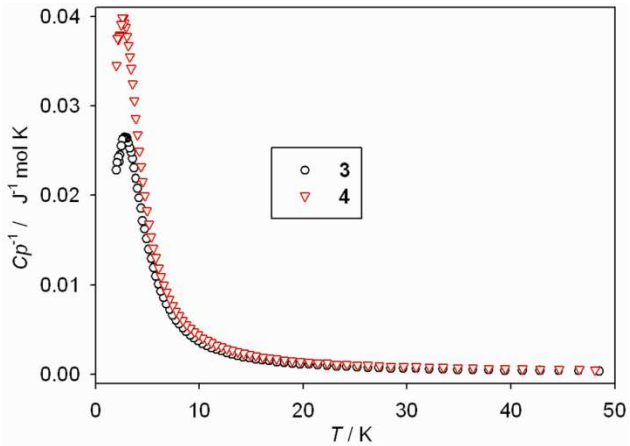

Figure 10 Temperature dependence of specific heat of complexes **3** (black circle) and **4** (red triangle).

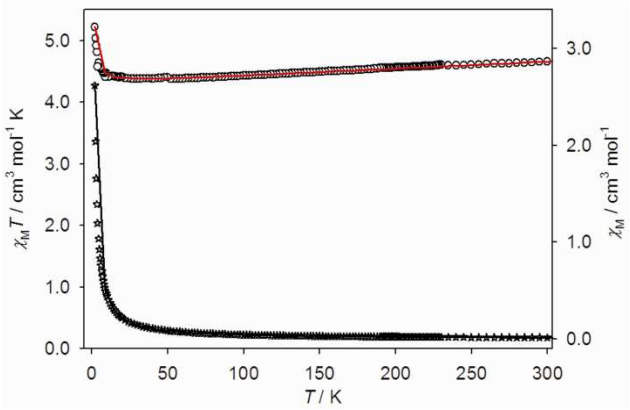

Figure 11 Magnetic behavior of complex **5** as measured in an applied field of 1000 Oe using a SQUID magnetometer. Fitting (black line) on χ_M *vs* T (star) and fitting (red line) on $\chi_M T$ *vs* T (circle) of complex **5** in the powder state.

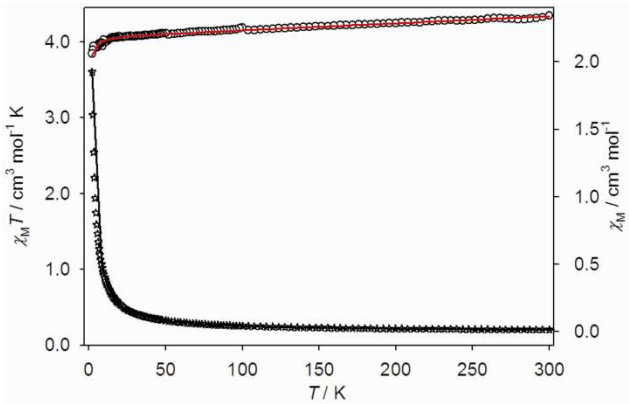

Figure 12 Magnetic behavior of complex **6** as measured in an applied field of 1000 Oe using a SQUID magnetometer. Fitting (black line) on χ_M *vs* T (star) and fitting (red line) on $\chi_M T$ *vs* T (circle) of complex **6** in the powder state.

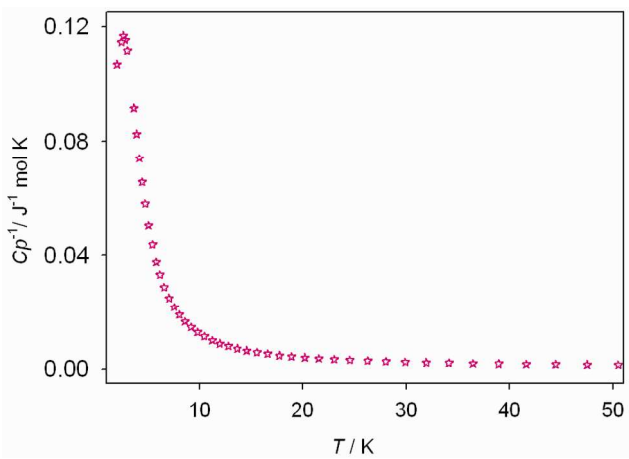

Figure 13 Temperature dependence of specific heat of complex **5**.

Notes and references

[a]*State Key Laboratory of Structure Chemistry, Fujian Institute of Research on the Structure of Matter, Chinese Academy of Sciences, Fuzhou, 350002, China. E-mail: tsheng@fjirsm.ac.cn.*
[b]*School of Chemistry and Chemical Engineering, University of Chinese Academy of Sciences, Beijing, 100049, China.*

† Electronic Supplementary Information (ESI) available: [X-ray crystallographic data in CIF format for complexes **1-6**]. See DOI: 10.1039/b000000x/

‡ Footnotes should appear here. These might include comments relevant to but not central to the matter under discussion, limited experimental and spectral data, and crystallographic data.

1. G. E. Pieslinger, P. Alborés, L. D. Slep and L. M. Baraldo, *Angew. Chem. Int. Ed.*, 2014, **53**, 1293; H. Oshio, H. Onodera and T. Ito, *Chem.-Eur. J.*, 2003, **9**, 3946; B. W. Pfennig, J. L. Cohen, I. Sosnowski, N. M. Novotny and D. M. Ho, *Inorg. Chem.*, 1999, **38**, 606; L. Dubicki, J. Ferguson, E. R. Krausz, P. A. Lay, M. Maeder, R. H. Magnuson and H. Taube, *J. Am. Chem. Soc.*, 1985, **107**, 2167.
2. S. Margadonna, K. Prassides and A. N. Fitch, *Angew. Chem. Int. Ed.*, 2004, **43**, 6316; P. Franz, C. Ambrus, A. Hauser, D. Chernyshov, M. Hostettler, J. Hauser, L. Keller, K. Kramer, H. Stoeckli-Evans, P. Pattison, H. B. Burgi and S. Decurtins, *J. Am. Chem. Soc.*, 2004, **126**, 16472; E. J. Schelter, F. Karadas, C. Avendano, A. V. Prosvirin, W. Wernsdorfer and K. R. Dunbar, *J. Am. Chem. Soc.*, 2007, **129**, 8139.
3. G. Rogez, A. Marvilliers, E. Riviere, J. P. Audiere, F. Lloret, F. Varret, A. Goujon, N. Mendenez, J. J. Girerd and T. Mallah, *Angew. Chem. Int. Ed.*, 2000, **39**, 2885.
4. D. M. D'Alessandro and F. R. Keene, *Chem. Rev.*, 2006, **106**, 2270; P. V. Bernhardt, F. Bozoglian, B. P. Macpherson and M. Martinez, *Coord. Chem. Rev.*, 2005, **249**, 1902; J. F. Endicott, P. G. McNamara, T. Buranda and A. V. Macatangay, *Coord. Chem. Rev.*, 2000, **208**, 61; C. Creutz and H. Taube, *J. Am. Chem. Soc.*, 1973, **95**, 1086; R. H. Magnuson, P. A. Lay and H. Taube, *J. Am. Chem. Soc.*, 1983, **105**, 2507.
5. X. Y. Wang, C. Avendano and K. R. Dunbar, *Chem. Soc. Rev.*, 2011, **40**, 3213; J. Černák, M. Orendáč, I. Potočňák, J. Chomič, A. Orendáčová, J. Skoršepa and A. Feher, *Coord. Chem. Rev.*, 2002, **224**, 51; M. Mikuriya, D. Yoshioka and M. Handa, *Coord. Chem. Rev.*, 2006, **250**, 2194; W. Oliver, *Coord. Chem. Rev.*, 2005, **249**, 2550.
6. O. Sato, A. Cui, R. Matsuda, J. Tao and S. Hayami, *Acc. Chem. Res.*, 2007, **40**, 361; M. D. Ward, *Chem. Soc. Rev.*, 1997, **26**, 365; S. i. Ohkoshi, H. Tokoro and K. Hashimoto, *Coord. Chem. Rev.*, 2005, **249**, 1830.
7. N. S. Hush, *Prog. Inorg. Chem.*, 1967, 391; N. S. Hush, *Coord. Chem. Rev.*, 1985, **64**, 135.
8. K. D. Demadis, C. M. Hartshorn and T. J. Meyer, *Chem. Rev.*, 2001, **101**, 2655; B. S. Brunschwig, C. Creutz and N. Sutin, *Chem. Soc. Rev.*, 2002, **31**, 168.
9. I. W. Chen, M. Fu, W. Tseng, J. Yu, S. Wu, C. Ku, C. Chen and S. Peng, *Angew. Chem. Int. Ed.*, 2006, **45**, 5814; M. Mitsumi, K. Kitamura, A. Morinaga, Y. Ozawa, M. Kobayashi, K. Toriumi, Y. Iso, H. Kitagawa and T. Mitani, *Angew. Chem. Int. Ed.*, 2002, **41**, 2767; H. Kitagawa, N. Onodera, T. Sonoyama, M. Yamamoto, T. Fukawa, T. Mitani, M. Seto and Y. Maeda, *J. Am. Chem. Soc.*, 1999, **121**, 10068; M. Mitsumi, T. Murase, H. Kishida, T. Yoshinari, Y. Ozawa, K. Toriumi, T. Sonoyama, H. Kitagawa and T. Mitani, *J. Am. Chem. Soc.*, 2001, **123**, 11179; M. Mitsumi, H. Ueda, K. Furukawa, Y. Ozawa, K. Toriumi and M. Kurmoo, *J. Am. Chem. Soc.*, 2008, **130**, 14102.
10. J. Brown, *Phil. Trans.*, 1724, **33**, 17; J. Woodward, *Phil. Trans.*, 1724, **33**, 15.
11. M. B. Robin, *Inorg. Chem.*, 1962, **1**, 337.
12. A. Ito, M. Suenaga and K. Ono, *J. Chem. Phys.*, 1968, **48**, 3597.
13. W. Liu, E. N. Nfor, Y. Z. Li, J. L. Zuo and X. Z. You, *Inorg. Chem. Commun.*, 2006, **9**, 923; R. Herchel, Z. Trávníček and R. Zbořil, *Inorg. Chem.*, 2011, **50**, 12390.
14. X. Ma, S. M. Hu, C. H. Tan, Y. H. Wen, Q. L. Zhu, C. J. Shen, T. L. Sheng and X. T. Wu, *Dalton Trans.*, 2012, **41**, 12163; X. Ma, C. S. Lin, S. M. Hu, C. H. Tan, Y. H. Wen, T. L. Sheng and X. T. Wu, *Chem.-Eur. J.*, 2014, **20**, 7025.
15. X. Ma, S. M. Hu, C. H. Tan, Y. F. Zhang, X. D. Zhang, T. L. Sheng and X. T. Wu, *Inorg. Chem.*, 2013, **52**, 11343.
16. A. A. Schilt, *J. Am. Chem. Soc.*, 1960, **82**, 3000.
17. A. A. Schilt, P. A. Russo and A. Wold, *Inorg. Synth.*, 1970, 247.
18. J. N. Demas, T. F. Turner and G. A. Crosby, *Inorg. Chem.*, 1969, **8**, 674.
19. E. M. Kober, J. V. Caspar, B. P. Sullivan and T. J. Meyer, *Inorg. Chem.*, 1988, **27**, 4587.
20. F. Lloret, M. Julve, M. Mollar, I. Castro, J. Latorre, J. Faus, X. Solans and I. Morgenstern-Badarau, *J. Chem. Soc., Dalton Trans.*, 1989, 729.
21. A. A. Schilte, *J. Am. Chem. Soc.*, 1963, **85**, 904.
22. G. Bryant, J. Fergusson and H. Powell, *Aust. J. Chem.*, 1971, **24**, 257.
23. G. M. Sheldrick, *SHELXL-97*, (1997) University of Göttingen, Germany
24. S. Z. Zhan, Q. J. Meng, X. Z. You, G. W. Wang and P. J. Zheng, *Polyhedron*, 1996, **15**, 2655.
25. F. Pan, Z. M. Wang and S. Gao, *Inorg. Chem.*, 2007, **46**, 10221.
26. C. A. Hunter and J. K. M. Sanders, *J. Am. Chem. Soc.*, 1990, **112**, 5525; M. L. Główka, D. Martynowski and K. Kozłowska, *J. Mol. Struct.*, 1999, **474**, 81.
27. C. A. Bignozzi, R. Argazzi, J. R. Schoonover, K. C. Gordon, R. B. Dyer and F. Scandola, *Inorg. Chem.*, 1992, **31**, 5260; B. J. Coe, T. J. Meyer and P. S. White, *Inorg. Chem.*, 1995, **34**, 3600.
28. A. A. Schilt, *Inorg. Chem.*, 1964, **3**, 1323.
29. C. A. Bignozzi, R. Argazzi, G. F. Strouse and J. R. Schoonover, *Inorg. Chim. Acta*, 1998, **275–276**, 380.
30. A. A. Schilt, *J. Am. Chem. Soc.*, 1960, **82**, 5779.
31. G. B. Shaw, C. L. Brown and J. M. Papanikolas, *J. Phys. Chem. A*,

2002, **106**, 1483; P. Byabartta, S. Pal, T. K. Misra, C. Sinha, F. L. Liao, K. Panneerselvam and T. H. Lu, *J. Coord. Chem.*, 2002, **55**, 479.
32. M. Srnec, J. Chalupský, M. Fojta, L. Zendlová, L. k. Havran, M. Hocek, M. r. Kývala and L. r. Rulíšek, *J. Am. Chem. Soc*, 2008, **130**, 10947; L. Rulíšek, *J. Phys. Chem. C*, 2013, **117**, 16871.
33. E. M. J. Johansson, M. Odelius, S. Plogmaker, M. Gorgoi, S. Svensson, H. Siegbahn and H. Rensmo, *J. Phys. Chem. C*, 2010, **114**, 10314.
34. N. K. Hamer and L. E. Orgel, *Nature*, 1961, **190**, 439.
35. E. M. Kober and T. J. Meyer, *Inorg. Chem.*, 1982, **21**, 3967.
36. M. B. Robin and P. Day, *Adv. Inorg. Chem.*, 1968, **10**, 247.
37. I. Šalitroš, R. Boča, R. Herchel, J. Moncol, I. Nemec, M. Ruben and F. Renz, *Inorg. Chem.*, 2012, **51**, 12755.
38. Z. Gu, Y. Xu, L. Kang, Y. Li, J. Zuo and X. You, *Inorg. Chem.*, 2009, **48**, 5073; A. M. Kutasi, D. R. Turner, P. Jensen, B. Moubaraki, S. R. Batten and K. S. Murray, *Inorg. Chem.*, 2011, **50**, 6673; K. J. Cho, D. W. Ryu, K. S. Lim, W. R. Lee, J. W. Lee, E. K. Koh and C. S. Hong, *Dalton Trans.*, 2013, **42**, 5796; L. C. Kang, X. Chen, H. S. Wang, Y. Z. Li, Y. Song, J. L. Zuo and X. Z. You, *Inorg. Chem.*, 2010, **49**, 9275; R. Lescouëzec, F. Lloret, M. Julve, J. Vaissermann, M. Verdaguer, R. Llusar and S. Uriel, *Inorg. Chem.*, 2001, **40**, 2065.
39. W. W. Ni, Z. H. Ni, A. L. Cui, X. Liang and H. Z. Kou, *Inorg. Chem.*, 2007, **46**, 22.
40. W. Hiller, J. Straehle, A. Datz, M. Hanack, W. E. Hatfield, L. W. Ter Haar and P. Guetlich, *J. Am. Chem. Soc.*, 1984, **106**, 329.
41. D. Visinescu, L. M. Toma, O. Fabelo, C. Ruiz-Pérez, F. Lloret and M. Julve, *Inorg. Chem.*, 2013, **52**, 1525; L. M. Toma, J. Pasan, C. Ruiz-Perez, F. Lloret and M. Julve, *Dalton Trans.*, 2012, **41**, 13716; E. Colacio, M. Ghazi, H. Stoeckli-Evans, F. Lloret, J. M. Moreno and C. Perez, *Inorg. Chem.*, 2001, **40**, 4876.
42. P. Seth, A. Figuerola, J. Jover, E. Ruiz and A. Ghosh, *Inorg. Chem.*, 2014, **53**, 9296; X. P. Shen, H. B. Zhou, J. H. Yan, Y. F. Li and H. Zhou, *Inorg. Chem.*, 2014, **53**, 116.
43. V. Comte and H. Vahrenkamp, *J. Organomet. Chem.*, 2001, **627**, 153.
44. D. F. Shriver and J. Posner, *J. Am. Chem. Soc.*, 1966, **88**, 1672.
45. C. A. Bignozzi, S. Roffia, C. Chiorboli, J. Davila, M. T. Indelli and F. Scandola, *Inorg. Chem.*, 1989, **28**, 4350.

Table of Content:

Syntheses, crystal structures, MMCT and magnetic properties of four one-dimensional cyanide-bridged complexes comprised of M^{II}-CN-Fe^{III} (M = Fe, Ru, Os)

Yong Wang,[a,b] Xiao Ma,[a] Shengmin Hu,[a] Zhenzhen Xue,[a,b] Yuehong Wen,[a] Xiaoquan Zhu,[a,b] Xudong Zhang,[a] Tianlu Sheng*,[a] and Xintao Wu[a]

[a] State Key Laboratory of Structure Chemistry, Fujian Institute of Research on the Structure of Matter, Chinese Academy of Sciences, Fuzhou, 350002, P. R. China

[b] School of Chemistry and Chemical Engineering, University of Chinese Academy of Sciences, Beijing, 100049, P. R. China

E-mail address: tsheng@fjirsm.ac.cn. Tel.: +086 (0)591 83792294.

Four 1D cyanide-bridged complexes [*cis*-$M^{II}(L)_2(CN)_2Fe^{III}$(salen)]($PF_6$) (**3-6**) have been synthesized, of which **3** and **4** are the Class II mixed-valence complexes.